Is comparison with experimental data a reasonable method of validating computational models?

V Timchenko[1*], S A Tkachenko[1], J Reizes[1], G E Lau[2], G H Yeoh[1]

[1]*School of Mechanical and Manufacturing Engineering, University of New South Wales, Sydney, NSW 2052, Australia*

[2]*BeeXergy Consulting Ltd, Unit 2608-09, APEC Plaza, 49 Hoi Yuen Road, Kwun Tong, Kowloon, Hong Kong SAR, China*

[*]v.timchenko@unsw.edu.au

Abstract. In the case of laminar flow, once all property variations are included, properly modelled and correctly solved a good agreement with experimental data means that numerical model has been validated. However, for turbulent flows the difference between experimental and numerical results could be the effect of an inadequate model or the use of inappropriate boundary conditions. A better agreement with the experiment, might be obtained by "improving" the model, or by obtaining "better" boundary conditions or a combination of the two. This issue is explored in the paper using the example of LES of buoyancy-driven flow in a tall rectangular cavity. Based on comparison with experimental data, it is shown that introducing heat losses through the top wall in simulations brings the numerical results closer to the experimental data. However, an improved subgrid model with all non-isothermal walls being adiabatic also brings numerical results and experimental data closer, at least near the hot wall. Therefore, experimental results cannot be used to validate numerical model of turbulent flows with heat transfer unless thermal boundary conditions can be established with reasonable accuracy.

1. Introduction

Since many problems acquired in computational fluid dynamics (CFD) require significant computational resources, one of the earliest decisions is how much the numerical model can be simplified to produce results that predict "reality" with sufficient "accuracy". One aspect of accuracy is routinely overcome by "grid refinement", to demonstrate that, at least as far as the numerical accuracy is concerned, the choice of the mesh and time step in the case of unsteady flow solutions, is based on the firm ground. It remains however, to demonstrate that the proposed model does predict results which are in "reasonable" agreement with numerical solutions of similar, previously solved problems, or, if available, experimental results. This is the validation problem.

In fluid mechanics and heat transfer the *only* way to determine the validity of a theory is to compare it with a "better" theory [1]. It should always be remembered that numerical solutions are approximate solutions and in the context of CFD a "better" theory is a solution which is based on fewer assumptions, or is in some ways more accurate. Unfortunately, in CFD "better solutions" are rarely available so that the agreement between a numerical solution and experimental data is usually considered as the "gold standard" and is usually accepted as the best indication that that the CFD model is predicting "correctly".

In most cases, the numerical model is simplified in two ways. One consists of the fluid flow equations used and the other is the system to be studied. For example, consider the apparently simple problem of the laminar flow in a two-dimensional differentially heated cavity with isothermal hot and cold walls and the top and bottom walls adiabatic. Firstly, a two-dimensional apparatus is impossible to build, but it could be argued that the flow on the centre vertical plane of the cavity might be acceptable as the flow to be matched. Secondly it is very difficult to physically produce absolutely "isothermal" walls and, finally, the so called adiabatic walls are usually characterised as "highly insulated," but obviously not adiabatic. The physical difference between the experimental "reality" and the numerical assumptions of isothermal and adiabatic boundaries are usually disregarded as being "small" in the interest of obtaining numerical solutions.

The simplest model is the Boussinesq Approximation in which all properties are considered constant except for the density in the buoyancy term of the momentum equation and radiative exchanges are completely neglected. When this model is used at low Rayleigh numbers with a linear variation in the density as a function of temperature, on the problem mentioned above, the centre of the resulting flow cell must occur at the centre of the cavity and the solution is anti-symmetric about the major diagonals of the cavity. Morrison and Tran [2] found experimentally that the centre of the cell moved towards the hot wall and up. They claimed that the reason for this drift was that the variation of transport properties with temperature was not taken into account in numerical models using the Boussinesq approximation.

When the variation of the transport properties was taken into account in the numerical model, Leonardi [3] found that the centre of the cell moved towards the cold wall and down, exactly the opposite result from that obtained by Morrison and Tran. Since there was no other variations that could be introduced to the equations, the only remaining difference had to be the boundary conditions used in the numerical solution. The insulation on the top boundary of the apparatus was then included in the model together with an assumed temperature in the laboratory and a correlation used for the evaluation of the Biot number on the surface. Now, the centre of the cell almost exactly matched the position found by Morrison and Tran [2]. This then, was proof that heat transfer through what has often been termed "inactive" walls can play a significant role and cannot be neglected. Similar problems of even greater complexity have been demonstrated by Leonardi *et al*. [3] in three-dimensional thermally driven flows.

In our experience when validation is discussed in the literature, the equations and the numerical procedures used to model the flow and heat transfer are the processes to be validated. In the case of the laminar flow discussed above, once all property variations had been included, properly modelled and correctly solved, no "better theory" can be found. However, unless a direct numerical simulation is employed (a computationally very expensive approach), whenever turbulent flows are studied, a model is required to overcome the closure problem. As a result, the validation of the CFD code becomes more difficult.

The differences between experimental and numerical results could be the effect of an inadequate model or the use of inappropriate boundary conditions. The "correct solution", that is indicated by the experiment, might be obtained by "improving" the model, or by obtaining "better" boundary conditions or a combination of the two. The question then arises as to whether the validation can identify the "appropriate model" to be used for the solution of such problems. This issue is explored in the paper based on the example of LES of buoyancy-driven flow in a tall rectangular cavity.

2. Computational model

2.1 Governing Equations

The computational model used in this study is based on the conservation equations for variable-property Newtonian fluids. To adequately model the transitional flow structures, a large-eddy simulation (LES) approach is adopted, in which the large-scale eddies are resolved explicitly and the

small-scale eddies are filtered and modelled. To account for the density variation within the flow, Favre-averaging is utilized, viz. $\tilde{\varphi}(\mathbf{x},t)=\overline{\rho\varphi(\mathbf{x},t)}/\bar{\rho}$, where $\varphi(\mathbf{x},t)$ is an any variable which is a function of time and space, $\bar{\rho}$ is the filtered density. Following from this, the density-based Favre-filtered mass, momentum, and energy conservation equations in Cartesian form can be written as:

$$\frac{\partial\bar{\rho}}{\partial t}+\frac{\partial\left(\bar{\rho}\tilde{u}_j\right)}{\partial x_j}=0 \tag{1}$$

$$\frac{\partial(\bar{\rho}\tilde{u}_i)}{\partial t}+\frac{\partial(\bar{\rho}\tilde{u}_i\tilde{u}_j)}{\partial x_j}=-\frac{\partial\bar{p}}{\partial x_i}+\frac{\partial}{\partial x_j}\left[\mu\left(\frac{\partial\tilde{u}_i}{\partial x_j}+\frac{\partial\tilde{u}_j}{\partial x_i}\right)-\frac{2}{3}\mu\frac{\partial\tilde{u}_k}{\partial x_k}\delta_{ij}\right]+\frac{\partial M_{ij}}{\partial x_j}+\left(\bar{\rho}-\rho_{ref}\right)\vec{g} \tag{2}$$

$$\bar{\rho}C_p\frac{\partial\tilde{T}}{\partial t}+\bar{\rho}C_p\tilde{u}_i\frac{\partial\tilde{T}}{\partial x_j}=\frac{\partial}{\partial x_j}\left(k\frac{\partial\tilde{T}}{\partial x_j}\right)+\frac{\partial q_j}{\partial x_j} \tag{3}$$

In Eqs. (1) – (3) ρ_{ref} is the reference density, $\tilde{u}$ is the filtered velocity vector, $\tilde{T}$ is the filtered temperature, μ is the dynamic viscosity, *Cp* is the specific heat of constant pressure and k is the thermal conductivity. In the present investigation, the dynamic viscosity is evaluated using the Sutherland equation [4] with the Sutherland constant *C* for air taken to be 120. In Eq. (3), the specific heat of constant pressure C_p is taken to be a polynomial function of temperature similarly to [10], and the thermal conductivity k is evaluated using $k = \mu C_p / \mathrm{Pr}$, in which Pr is the Prandtl number of air.

In LES, the effect of small-scale eddies is taken into account in the conservation equations via the subgrid-scale (SGS) stress tensor M_{ij} as shown in Eq. (2) and the flux vector $\mathbf{q}$ in Eq. (3). M_{ij} is modelled as

$$M_{ij}=\overline{\tau}_{u_iu_j}-\frac{1}{3}\tau_{kk}\delta_{ij}\approx-2\mu_t\left(\tilde{S}_{ij}-\frac{1}{3}\tilde{S}_{kk}\delta_{ij}\right) \tag{5}$$

where μ_t is the SGS viscosity, $\left|\tilde{S}\right|=\sqrt{2\tilde{S}_{ij}\tilde{S}_{ij}}$ and $\tilde{S}_{ij}=\frac{1}{2}\left(\frac{\partial\tilde{u}_i}{\partial x_j}+\frac{\partial\tilde{u}_j}{\partial x_i}\right)$. Since natural convection in a cavity can be considered as a weakly compressible flow, $\tilde{S}_{kk}\delta_{ij}$ may be ignored [5]. The SGS thermal flux vector $\mathbf{q}$ is typically modelled using the SGS Prandtl number, Pr_t, based on the formulation of Eidson [6] which given the components of $\mathbf{q}$ as

$$q_j=\bar{\rho}\left(\widetilde{u_jT}-\tilde{u}_j\tilde{T}\right)\approx-\frac{\mu_t}{\mathrm{Pr}_t}\frac{\partial\tilde{T}}{\partial x_j} \tag{6}$$

The closure of the equations Eq. 5 and 6 requires a model for the SGS viscosity μ_t. In the present work, it is modelled using the Vreman [7] formulation (VM), in which $\mu_t = \rho\ C_v\ \Pi_g$, where $\Pi_g=\sqrt{\frac{B_\beta}{\alpha_{ij}\alpha_{ij}}}$, $\alpha_{ij}=\frac{\partial\tilde{u}_j}{\partial x_i}$ is a 3x3 matrix of velocity derivatives, $\beta_{ij}=\Delta_m^2\alpha_{mi}\alpha_{mj}$, $B_\beta=\beta_{11}\beta_{22}-\beta_{12}\beta_{12}+\beta_{11}\beta_{33}-\beta_{13}\beta_{13}+\beta_{22}\beta_{33}-\beta_{23}\beta_{23}$, and Δ_m is the filter width of subgrid in the direction *m*. This SGS model is preferable to the Smagorinsky model [8] as the latter has been found to be too dissipative for simulations of wall-bounded shear flows [9]. In contrast to the Smagorinsky model, the Vreman model has been found to predict zero dissipation in regions in which the flow is laminar, hence giving more accurate predictions of the location of transition [10].

Although VM has been shown to be successful in predicting many turbulent and transitional flows [11], its model coefficient was found to be insufficient to adapt to the flow. You and Moin [12] utilized the energy equation on the basis of internal energy to derive an expression for Pr_{sgs}. Following

this approach, the present co-workers [13] adapted a "global equilibrium" dynamic procedure into the Vreman model (DVME) for the flows at low Mach numbers in which compressibility effects due to propagation of acoustic waves may be ignored. It was demonstrated that this formulation is applicable to correctly capture the location of transition in a boundary layer in natural convective flows. Details of this formulation can be found in [13].

2.2 Numerical Methodology

Finite volume method (FVM) is utilized to discretize the filtered transport equations on a collocated grid. The convective terms are approximated using 4th-order central differencing scheme whereas the diffusion terms as well as other spatial derivatives are approximated using the 2nd-order central differencing scheme. The numerical solution is advanced in time using an explicit two-step predictor-corrector approach, which involves a 2nd-order Adams-Bashforth time integration scheme for the predictor stage and a 2nd-order quasi Crank-Nicolson integration scheme for the corrector stage. Pressure correction steps which are incorporated in both the predictor and corrector stages involve the inversion of pressure correction Poisson equations and are solved by means of Krylov methods. Detailed derivation and implementation of the numerical method in the in-house code can be found in Lau et al. [10]. In all cases, simulations were carried out for approximately 25 000 time steps before sampling of the turbulent data was begun. Stability of the numerical algorithm was ensured by employing a maximum Courant–Friedrichs–Lewy (CFL) criterion of 0.35 in all simulations with a maximum time step of 0.005s.

2.3 Computational domain and boundary conditions

The configuration studied is a differentially heated enclosed rectangular cavity [14, 15] used in the experimental study by King [15]. The dimensions of the cavity are width (*W)* × height (*H*) × depth (*D*) are 0.5 m × 2.5 m × 1.0 m. The temperature difference between the hot and cold walls was 45.8°C, giving Ra = 4.56×10^{10}. Since silicon heaters were used to maintain the temperatures of the hot and cold walls, it is reasonable to assume that these temperatures were constant during the experiment. All other walls were insulated with expanded polystyrene. A more detailed description of the experimental apparatus can be found King's PhD thesis [15].

The 3-D computational domain used to replicate this experiment in the present study together with the frame of reference is shown in figure 1(a). A non-uniform mesh has been adopted with a finer mesh positioned in near-wall regions to capture accurately the boundary layer physics. Three grid resolutions were tested in the present study. It was shown that the coarse mesh (75, 163, 78) was sufficient to resolve the viscous sublayer of the turbulent boundary layer as the first mesh point is located within $x^+ < 1.1$. The differences between the time averaged numerical results obtained using the medium and fine grids were found to be small. Thus in the following, numerical results are presented for the fine mesh.

For the velocities no-slip boundary condition was applied at all solid walls. A Dirichlet boundary condition was applied for the temperature at the isothermal walls with the hot wall, T_H = 350.35 K and the cold wall, T_C = 304.55 K. In the case of well-insulated walls all solid walls were assumed as being adiabatic, so that the Neumann boundary condition, $\partial T/\partial n = 0$, in which n is normal to a wall, was applied at the top, bottom and side walls.

In order to investigate the effect of heat loss through the top wall on the nature of transition onset in the flow and thermal boundary layers, a 1-D approach was adopted to estimate the heat loss through the top wall of the cavity. The thickness of the expanded polystyrene employed by King [15] was 0.205 m, and its thermal conductivity was assumed $k_s = 0.033$ W/mK. The heat transfer rate was calculated at every time step from the internal wall temperature of the cavity $\tilde{T}_{w,i}$ and the ambient temperature around the apparatus, by writing energy balance equations for fluid, solid and ambient conditions: $k\,\partial T/\partial y|_{\text{cavity}} = k_s\,\partial T/\partial y|_{\text{solid}}$, and $k_s\,\partial T/\partial y|_{\text{solid}} = h_{air}\,(T_{w,o}-T_{amb})$, as illustrated on figure 1(b).

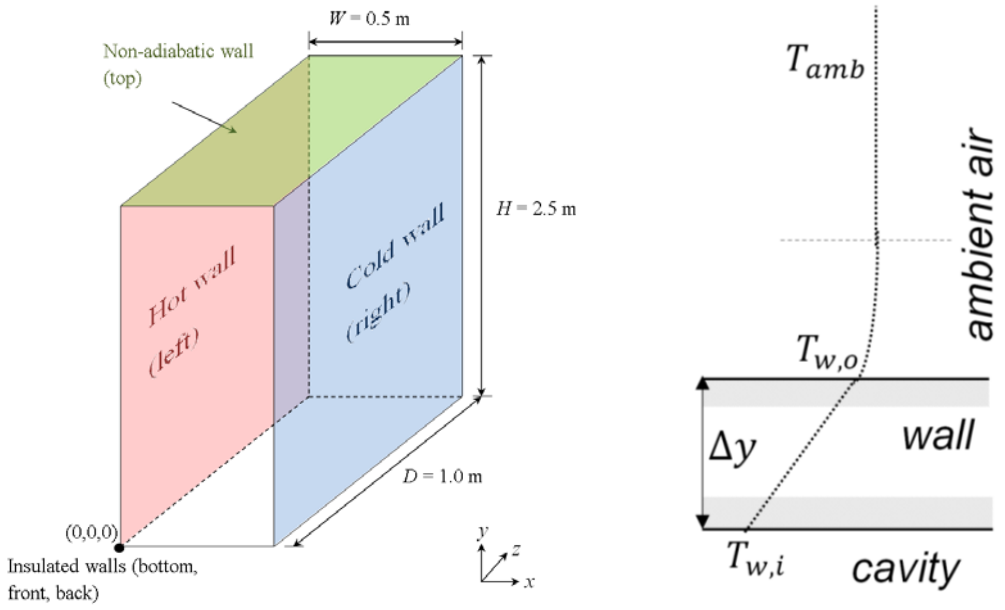

(a) (b)

Figure 1. (a) Computational domain, (b) The heat loss model at the top wall (polystyrene).

The ambient temperature was assumed $T_{amb} = 288.15\text{K}$, and two values of the heat external convective heat transfer coefficients of $h_{\text{air}} = 10$ W/(m^2 K) and $h_{\text{air}} = 15$ W/(m^2 K) representing typical values for natural convection were assumed.

3. Results and discussion

The mean temperature and vertical velocity profiles in the central x–y plane at two locations along the height of the cavity are shown in figures 2(a, b). As might be seen in figure 2(a) at mid-height, Y/H=0.497, in the case of the top wall being adiabatic the DVME model is in better agreement with the experiment than the non-dynamic Vreman model (VM) with the discrepancy in the temperature values reduced by 7% on the average. However, when heat losses from the top wall are taken into account, even better agreement with experimental results was obtained with average discrepancy between experimental and numerical temperature values in the middle of the cavity reduced to 43% of the VM discrepancy. The difference between using h=10 and 15 W/(m^2 K) is insignificant. For the velocity values, figure 2(b), the difference between experimental data and numerical results is reduced by 36% using DVME instead of VM with an adiabatic boundary conditions, whereas the discrepancy is halved when VM is used with a non-adiabatic top wall for both heat transfer coefficients.

Near the top of the cavity, Y/H=0.765, there is less than 1% change on the average between DVME and VM results. The non-adiabatic VM results for h=15 W/ m^2 K only slightly improve, 9%, the numerical results for the temperature field, whilst with h=10 W/ m^2 K a more significant improvement of 27% occurs. The differences in the velocity profiles near the top of the cavity are similar to each other, with the non-adiabatic boundary conditions yielding results slightly closer to the experimental data.

Figure 2(c) displays the time-averaged Nusselt number distribution along both the hot and cold walls at the centreline i.e. z/D = 0.5 of the cavity. In the present study, the Nusselt number is computed as $\text{Nu} = (\partial T/\partial x)_{wall} \cdot H / (T_H - T_C)$. It can be seen that the introduction of heat loss at the top wall improves prediction of the Nusselt number considerably including the shift in the gradient of the profile which is often used to indicate flow transition, at about y/H = 0.4. This is consistent with the results presented in figure 3, 4, in which heat loss introduced at the top wall has been found to enhance the turbulent activity and flow mixing in the cavity. From figure 2(c) it also can be seen that DVME better predicts transition in natural convective boundary layer than VM.

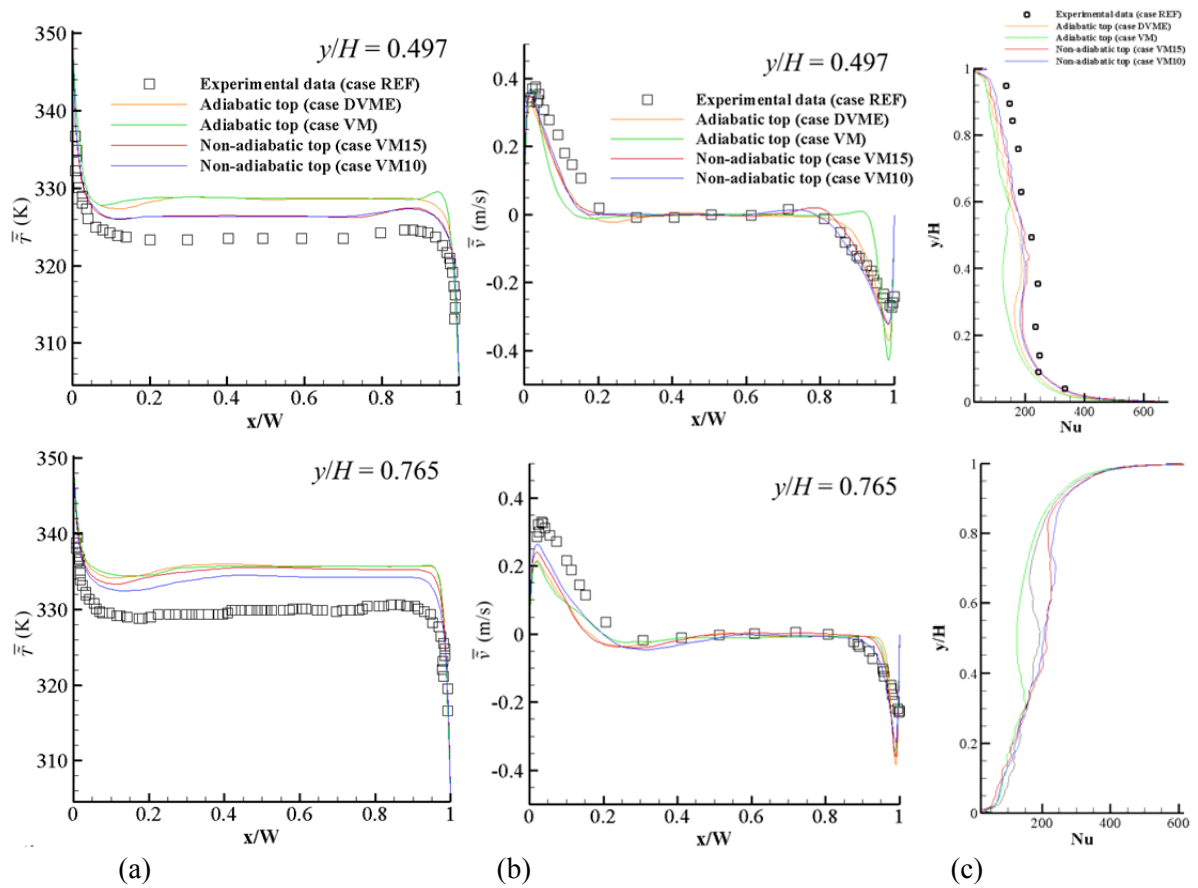

Figure 2. (a-b) Comparison of the time-averaged (a) temperature profiles and (b) v-velocity profiles with experimental data at the central plane z/D = 0.5 (c) Time-averaged Nusselt number distribution along the height of the cavity at z/D = 0.5 on the cold wall (top) and cold wall (bottom).

A comparison of the evolution of rms *v*-velocity fluctuations $\sqrt{v'^2}$ (figure 3(a)) and of the vertical turbulent heat flux $\overline{v'T'}$ (figure 3(b)) along the height of the cavity at the central *x*-*y* plane is presented between numerical results and experimental data in figure 3. It is clear that the fluctuations at the cold wall near the top of the cavity are considerably under-predicted when of either VM and DVME is used with an adiabatic top wall, as indicated by peaks of the profiles at $y/H = 0.765$ as well as by the spread of the profiles which are not well captured in these cases. On the contrary, both cases with non-adiabatic wall give reasonably good predictions of the turbulent quantities at this location. This is consistent with the results for the λ_2 criterion presented in figure 4. The vortex cores visualised by using this criterion clearly indicate the differences between the various models.

It is clear the VM subgrid model, figure 4(a), generates greater levels of turbulence than the DVME model shown in figure 4(b). As discussed above, this leads to better agreement with experimental results on the hot wall with the DVME model than with the VM model. However, both models perform poorly on the cold wall when compared with experimental results. Part for the reason for the poor performance of the two models is the level relaminarisation of the flow on the on the top wall, with both models apparently having too much damping. As may be seen in comparing figure 4(c) with figures 4(a) and 4(b), the damping of fluctuations is on the top wall is reduced when heat losses are included in the VM model, but the level of damping is dependent on the heat transfer through the top wall as show in figures 4(c) and 4(d). In both these figures the transition point is closer to the corner than in case VM and agreement with experiment is better, though by no means perfect.

As would have been expected the numerical results are dependent on both the model used and the boundary conditions. Since natural convection is driven by temperature differences, it is well known that seemingly small differences in boundary conditions can result in significantly differing flows. In this particular case, the introduction of heat transfer through the top boundary increases agreement with experimental results of the VM model to a greater extent than changing the model to DVME. The question now arises, unless the experimental boundary conditions are sufficiently well known, can one subgrid model be said to be better than another when the numerical solutions are compared with experimental measurements? This means that experimental data needs to be used with caution in evaluating the performance of a numerical scheme.

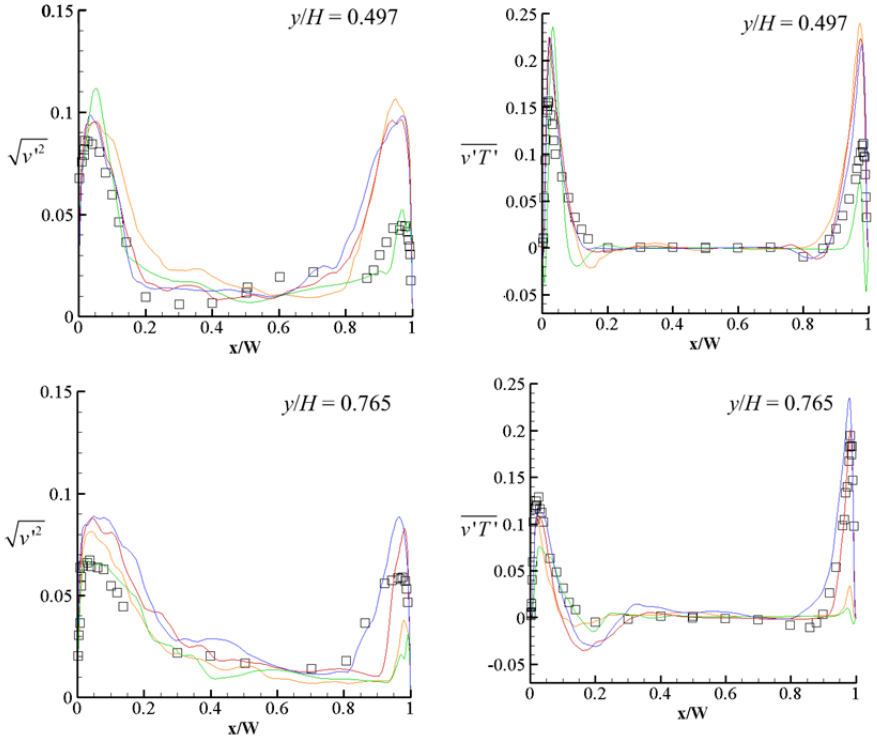

Figure 3. Comparison of the (a) rms *v*-velocity fluctuations and (b) of the vertical turbulent flux with experimental data at the central plane *z/D* = 0.5

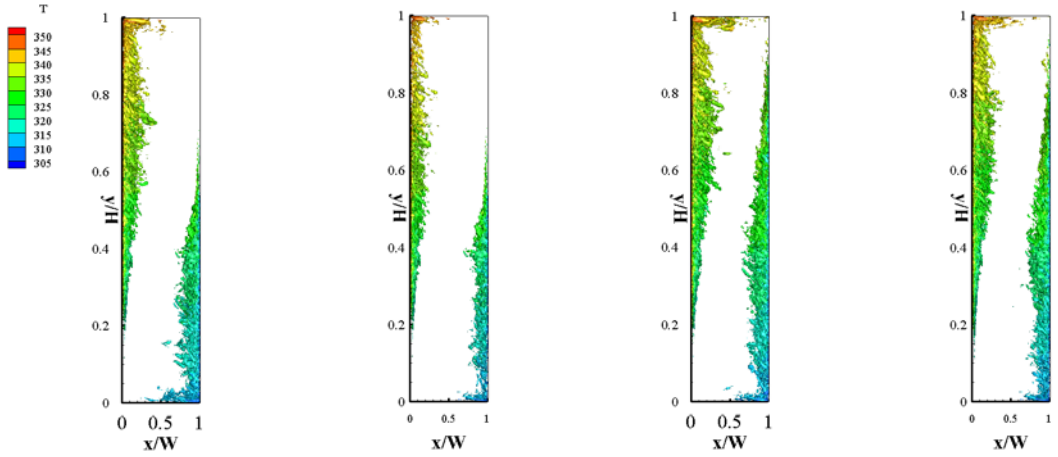

Figure 4. 3-D isosurfaces of λ_2 at the *z/D* = 0.5 plane colored by T for cases (a)VM, (b) DVME, (c) VM10, (d) VM15.

3. Conclusion

Comparison of CFD results with experiment is usually used as *the* means of validating the numerical model for velocity and temperature fields of the fluid. It is shown that this approach is correct for laminar flows calculated with all properties variable. The cause for differences between numerical and experimental results can only be the boundary conditions. However, the validation of turbulence models is more complex. It is shown that the agreement between numerical models and experimental date can be improved by employing a "better" numerical model or more realistic boundary conditions. Unless the "correct" thermal boundary conditions are employed it cannot be said that the CFD model has been validated even if the numerical and experimental results agree exactly. It follows that if experimental results be used for the validation of CFD codes involving heat transfer in turbulent flows, sufficient information about the experiment must be present to allow a reasonable evaluation of the boundary conditions or these must be given.

REFERENCES

[1] T.Fink 1970 Personal communication.
[2] Morrison G L *et al.* 1978 Laminar flow structure in vertical free convective cavities. *International Journal of Heat and Mass Transfer* **21**(2): p. 203-213.
[3] Leonardi E *et al.* 1999 Effects of finite wall conductivity on flow structures in natural convection, paper at CHMT1999. *Proceeding of the inter. Confer. on computational Heat and Mass Transfer, Cyprus*: p. 26-29.
[4] Sutherland W 1893 LII. The viscosity of gases and molecular force. *The London, Edinburgh, and Dublin Philosophical Magazine and Journal of Science* **36**(223): p. 507-531.
[5] Erlebacher G *et al.* 1992 Toward the large-eddy simulation of compressible turbulent flows. *Journal of Fluid Mechanics* **238**: p. 155-185.
[6] Eidson T M 1985 Numerical simulation of the turbulent Rayleigh–Bénard problem using subgrid modelling. *Journal of Fluid Mechanics* **158**: p. 245-268.
[7] Vreman A W 2004 An eddy-viscosity subgrid-scale model for turbulent shear flow: Algebraic theory and applications. *Physics of Fluids (1994-present)* **16**(10): p. 3670-3681.
[8] Smagorinsky J 1963 General circulation experiments with the primitive equations: I. the basic experiment*. *Monthly weather review* **91**(3): p. 99-164.
[9] Barhaghi D G *et al.* 2006 Large-eddy simulation of natural convection boundary layer on a vertical cylinder. *International journal of heat and fluid flow* **27**(5): p. 811-820.
[10] Lau G *et al.* 2011 Large-eddy simulation of turbulent natural convection in vertical parallel-plate channels. *Numerical Heat Transfer, Part B: Fundamentals* **59**(4): p. 259-287.
[11] Vreman A W *et al.* 2009 A similarity subgrid model for premixed turbulent combustion. *Flow Turbulence Combustion* **82**: p. 233-248.
[12] You D *et al.* 2008 *A dynamic global-coefficient subgrid-scale model for compressible turbulence in complex geometries*. in *Annual Research Briefs*. 2008. Center for Turbulence Research, Standford University.
[13] Lau G E *et al.* 2012 Application of dynamic global-coefficient subgrid-scale models to turbulent natural convection in an enclosed tall cavity. *Physics of Fluids* **24**: p. 094105.
[14] Cheesewright R *et al.* 1986 Experimental data for the validation of computer codes for the prediction of two-dimensional buoyant cavity flows, in *ASME Winter Annual Meeting, HTD-60, Anaheim*.
[15] King K J 1989 Turbulent natural convection in rectangular air cavities. *Queen Mary College, University of London, London*.